Frequency shifting for acoustic feedback reduction

Jan Scheuing and Bin Yang
Chair of System Theory and Signal Processing
University of Stuttgart, Germany

{jan.scheuing, bin.yang}@Lss.uni-stuttgart.de

Abstract

Acoustic feedback is a well-known phenomenon in any electro-acoustical real-time system. Whenever the loop gain of a system exceeds 1 for any frequencies, the system becomes unstable: Feeding the amplified sound signal back into the microphone causes a penetrating whistle. Among others, one concept to reduce acoustic feedback is frequency shifting. The implementation of a frequency shifter is easy by using analog circuits, but quite demanding for digital real-time applications like digital audio mixers. This paper describes the theoretical background and our real-time implementation on a TI TMS320C5416.
We used the complex FIR filter approach for analytic signal generation in order to ensure equal amplitude response and constant group delay in the real and imaginary signal path. At a sampling frequency of $f_S = 24$ kHz we got satisfactory results with a group delay of about 10 ms which is short enough for real-time systems.

1 Introduction

As sonic power generated by the human voice is usually too small for stage applications, an electro-acoustical system consisting of at least one microphone, one amplifier, and one loudspeaker is used. Acoustical feedback appears whenever in a common environment microphones and loudspeakers are connected directly. Humans don't sense a small rate of feedback consciously. A predominant feedback in contrast is annoying.

Figure 1 shows the above mentioned minimal electro-acoustical system. The signal $s(t)$ of the speaker is received at the microphone and is emitted by the loudspeaker after amplification by $G(\omega)$. The emitted signal $l(t)$ is received by the listener and also contributes to the microphone signal $m(t)$.

For the following analysis, we assume that all components and transmission channels in this system are linear and time-invariant and can be described by the frequency responses $H_{xy}(\omega)$ with x and y being S for speaker, M for microphone, L for loudspeaker, and Z for listener.

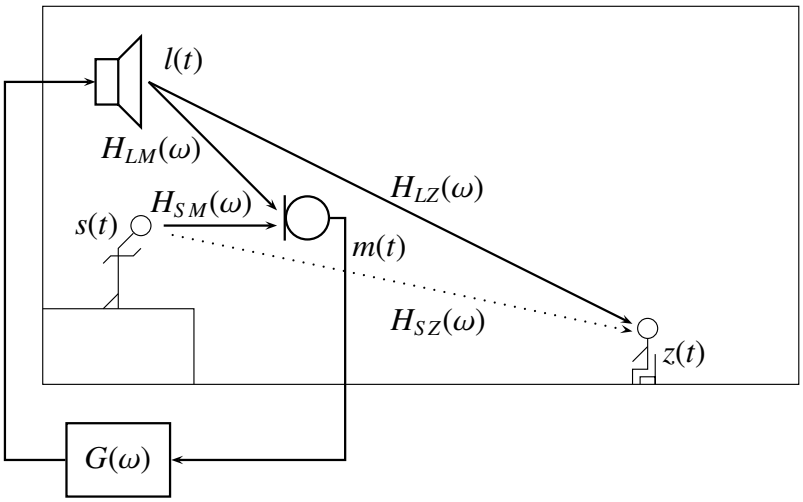

Figure 1: Acoustical transmission in stage applications

The input-output-behavior of the system can be expressed in frequency domain by

$$Z(\omega) = \underbrace{\Big(H_{SZ}(\omega) + H_{SM}(\omega)\,G(\omega)\Big(1 + G(\omega)H_{LM}(\omega) + G^2(\omega)H_{LM}^2(\omega) + \ldots\Big)H_{LZ}(\omega)\Big)}_{F(\omega)}\,S(\omega) \quad (1)$$

To simplify the analysis, we assume that the speaker talks directly into the microphone (leading to $H_{SM}(\omega) = 1$) and that the direct acoustical transmission from speaker to listener is neglectable ($H_{SZ}(\omega) = 0$). Therefore, (1) leads to

$$F(\omega) = G(\omega)\Big(1 + G(\omega)H_{LM}(\omega) + G^2(\omega)H_{LM}^2(\omega) + \ldots\Big)H_{LZ}(\omega), \quad (2)$$

which converges for $|G(\omega)H_{LM}(\omega)| < 1$ to

$$F(\omega) = \frac{G(\omega)H_{LZ}(\omega)}{1 - G(\omega)H_{LM}(\omega)}. \quad (3)$$

An exemplary Nyquist plot of the loop gain $G(\omega)H_{LM}(\omega)$ for audible frequencies is shown in figure 2. Considering a small loop gain, the microphone signal $m(t)$ does not differ significantly from the speaker signal $s(t)$. Increasing amplification in $G(\omega)$ corresponds to a dilation of the Nyquist plot. If the loop gain encloses the value 1, the system will become unstable. Starting from about 3 dB below that critical amplification, feedback is audible [1].

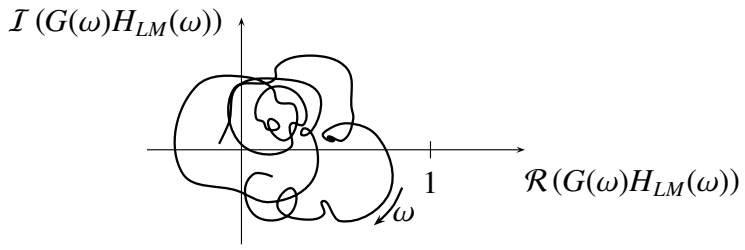

Figure 2: Nyquist plot of the loop gain

For stage applications there are two main categories of feedback reduction methods: equalization and periodic phase modulation. The former category includes all methods that choose $G(\omega)$

such that $|G(\omega)H_{LM}(\omega)|$ is smaller than one for all frequencies. This was first mentioned in [2] and is nowadays done by hand or implemented adaptively. In this paper, we will concentrate on the latter category. Section 2 presents a short introduction to periodic phase modulation. In section 3, we compare three strategies of frequency shifting. Finally, our implementation is discussed in details in section 4.

2 Acoustic feedback reduction using periodic phase modulation

Acoustic feedback arises at particular spectral components having a gain loop near 1 that experience at each loop cycle the same favorable phase conditions. Modulating the phase of the signal disturbs these optimal phase conditions [3, 4].

Phase modulation in this content means something different than phase modulation in digital communication. The microphone signal is not the modulation function of some carrier frequency, but rather the "carrier signal" modulated by some phase function. The modulated signal $y(t)$ is derived by

$$y(t) = x(t)\, \mathrm{e}^{\mathrm{j}\Phi(t)} \tag{4}$$

where $x(t)$ is the analytic version of the input signal and $\Phi(t)$ is the modulation function. A phase modulator is linear and time-variant. A periodic phase modulator is periodically time-variant [5].

There were several suggestions for feedback reduction using phase modulation. Guelke and Broadhurst proposed a sinusoidal modulation function [1]. Sinusoidal phase modulation or delay modulation were also suggested. The paper [4] presents a good overview.

In the following, we will concentrate on the frequency shifting proposed by Schroeder [6]. At each loop cycle the frequency of the emitted signal is shifted by Δf in the range of a few Hz. Due to periodicity of the phase, frequency shifting is also a periodical phase modulation with

$$\Phi(t) = 2\pi\, \Delta f t = \Delta\omega\, t. \tag{5}$$

Phase modulation causes some distortions to the signal: Sinusoidal phase and frequency modulation imply an additional amplitude modulation. Frequency shifting changes the interval of two tones. Choosing the modulation parameter $\Delta\omega$ is therefore a compromise between sufficient feedback reduction and imperceptible distortion.

3 Digital implementation

There exist several strategies for a digital implementation of frequency shifters. Below we describe and compare three possibilities.

3.1 Emulation of analog frequency shifting

Frequency shifting can easily be realized in analog technique by twice mixing the input signal and appropriate lowpass filtering to avoid aliasing, see figure 3. Both carrier frequencies are

larger than half of the bandwidth ω_B of the microphone signal. They differ in $\Delta\omega$ which is the desired frequency shift.

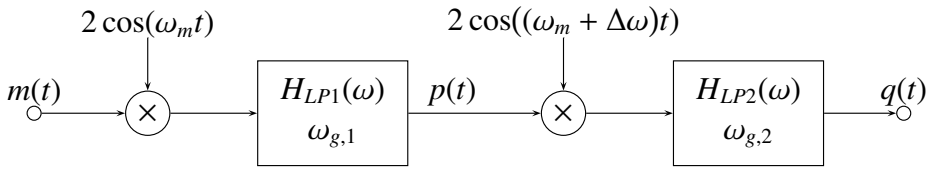

Figure 3: Block diagram of an analog implementation

The output signal can be described in the frequency domain by

$$\begin{aligned} P(\omega) &= H_{LP1}(\omega)[M(\omega-\omega_m)+M(\omega+\omega_m)] \\ Q(\omega) &= H_{LP2}(\omega)[P(\omega-\omega_m-\Delta\omega)+P(\omega+\omega_m+\Delta\omega)] \end{aligned} \tag{6}$$

Assuming an ideal lowpass $H_{LP1}(\omega) = \begin{cases} 1, & |\omega| \le \omega_{g,1} \\ 0, & \text{otherwise} \end{cases}$ and $\omega_{g,1} = \omega_m \ge \frac{\omega_B}{2}$, we obtain the desired frequency shifted signal

$$Q(\omega) = H_{LP1}(\omega-\omega_m-\Delta\omega)M(\omega-\Delta\omega) + H_{LP1}(\omega+\omega_m+\Delta\omega)M(\omega+\Delta\omega). \tag{7}$$

The lowpass H_{LP2} is used to reject the spectrum images around $\pm\omega_m$. The requirements on its filter design are much lower. We may emulate the described analog circuit by a digital system. Besides the high slew rate in H_{LP1}, the sampling frequency needs to fulfill $\omega_A > 2\omega_m$, which means an oversampling of the microphone signal by a least a factor of 2 and therewith a higher data rate.

3.2 Method using discrete Fourier transform

Another method may be depicted as "shifting the energy bins in frequency domain". The input signal $m(t)$ is sampled at ω_A. Then the input samples $m(n)$ are subdivided into blocks $m_b(n)$ of length L such that

$$m(n) = \sum_b m_b(n - bL). \tag{8}$$

Each signal block $m_b(n)$ will be windowed and zero-padded resulting to a block $\tilde{m}_b(n)$ of length $N \ge L$. It is then transformed to the frequency domain, e.g. by FFT,

$$M_b(k) = \sum_{n=0}^{N-1} \tilde{m}_b(n)\, \mathrm{e}^{-\mathrm{j}\frac{2\pi}{N}kn} \tag{9}$$

In this case, a power of 2 should be chosen for N. $M_b(k)$ contains samples of the Fourier transform at the analog frequency bins

$$\left[0, \frac{\omega_A}{N}, \ldots, \frac{(N/2-1)\,\omega_A}{N}, -\frac{\omega_A}{2}, -\frac{(N/2-1)\,\omega_A}{N}, \ldots, -\frac{\omega_A}{N}\right]. \tag{10}$$

Frequency bins may now be moved by any integer number of $\frac{\omega_A}{N}$ to generate the output signal: A positive frequency shift $\Delta\omega = +\frac{\omega_A}{N}$, corresponding to one step of bin movement, is realized by

$$Q_b(k) = \left[0, M_b(0), \ldots, M_b(\frac{N}{2} - 2), M_b(\frac{N}{2} + 1), \ldots, M_b(N-1), 0\right] \tag{11}$$

and a negative frequency shift $\Delta\omega = -\frac{\omega_A}{N}$ is realized by

$$Q_b(k) = \left[M_b(1), \ldots, M_b(\frac{N}{2} - 1), 0, 0, M_b(\frac{N}{2}), \ldots, M_b(N-2)\right]. \tag{12}$$

Upper and lower frequency bins are truncated. This is neglectable for usual shifting frequencies of $|\Delta f| < 15$ Hz with speech signals. Finally, the output signal $q(n)$ is obtained by inverse Fourier transform and overlap-add of $Q_b(k)$.

The main drawback of this strategy is its large latency. The FFT length N should be high in order to obtain a sufficiently small frequency shift: N should be e.g. 4096 at $f_S = 24$ kHz for a granularity of about 6 Hz in frequency shift. On the other hand, the corresponding high block length L leads to a long system latency. If $L = N$, the delay due to block processing is $\frac{4096}{24\text{ kHz}} = 170$ ms which is unacceptable in most applications.

3.3 Phase modulation using a complex FIR filter

According to section 2, frequency shifting may be interpreted as periodic phase modulation. Therefore, the analytical version $\tilde{m}(n)$ of the input sequence $m(n)$ is multiplied by the time-varying complex phase factor $\exp(\mathrm{j}\frac{\Delta\omega}{\omega_A}n)$. The real part of this product is the wanted frequency shifted signal

$$q(n) = 2\,\mathcal{R}\left\{\tilde{m}(n)\,\mathrm{e}^{\mathrm{j}\frac{\Delta\omega}{\omega_A}n}\right\} = 2\,\mathcal{R}\{\tilde{m}(n)\}\,\cos\left(\frac{\Delta\omega}{\omega_A}n\right) - 2\,\mathcal{I}\{\tilde{m}(n)\}\,\sin\left(\frac{\Delta\omega}{\omega_A}n\right). \tag{13}$$

In order to avoid block processing, analytic continuation of $m(n)$ may be achieved by a Hilbert filter with the ideal impulse response

$$h_{\mathrm{Hilb,id}}(n) = \begin{cases} 0, & n = 0 \\ \frac{1}{\pi n}, & \text{otherwise} \end{cases}, \tag{14}$$

that returns sample-by-sample the corresponding imaginary part of $m(n)$. Causal Hilbert filters may be approximated by IIR or FIR filters with the impulse responses

$$h_{\mathrm{Hilb,IIR}}(n) = \begin{cases} 0, & n < 0,\ n = d \\ \frac{1}{\pi(n-d)}, & \text{otherwise} \end{cases} \quad \text{and} \quad h_{\mathrm{Hilb,FIR}}(n) = \begin{cases} 0, & n < 0,\ n > 2d,\ n = d \\ \frac{1}{\pi(n-d)}, & \text{otherwise} \end{cases}. \tag{15}$$

In order to be synchronous, the real part $\mathcal{R}\{\tilde{m}(n)\}$ must also be delayed by d.

The causality approximation leads to a non-rectangular magnitude response in the imaginary path. Combined with the phase shift in (13), this causes artefacts in the output signal and is the main reason for choosing the following complex filter approach instead.

An ideal filter to generate the analytic signal $\tilde{m}(n)$ from its real valued counterpart $m(n)$ may be computed by shifting an ideal $\frac{\omega_A}{4}$-lowpass by $\frac{\omega_A}{4}$ in frequency [7]. In this way, a complex

filter is designed starting from a somehow approximated $\frac{\omega_A}{4}$-lowpass, whose filter coefficients are multiplied by $e^{j\frac{\pi}{2}n}$. This complex filter approximately returns the real and imaginary part of the analytic continuation of its real-valued input signal. Magnitude responses of the real and imaginary path as well as their group delays are always equal by construction. They only depend on the lowpass filter approximation.

As we are only interested in the real part of the complex multiplication result, half of the computation effort can be saved, see (13). The total system is shown in figure 4.

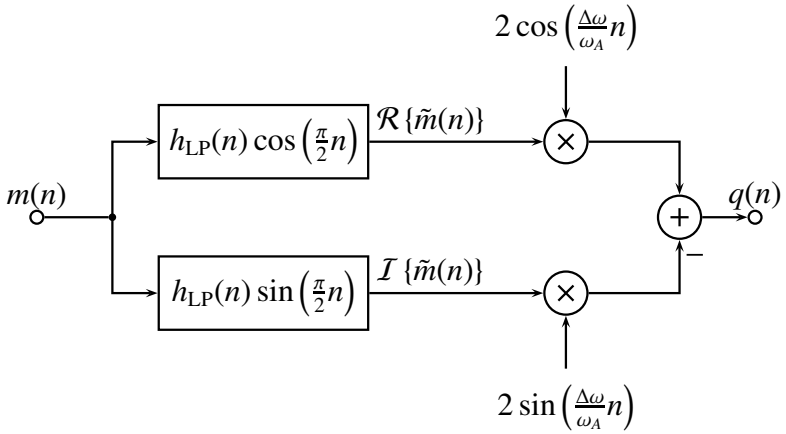

Figure 4: Block diagram of frequency shift

We choose a linear phase FIR filter for the lowpass in order to have a constant group delay for all frequencies. For a comparable quality of the frequency shifted output signal, the latency is much shorter compared to the second method in section 3.2. It is about 10 ms for an FIR filter of length $N = 512$ at $f_S = 24$ kHz.

The designed linear phase FIR lowpass must be of type II with an even impulse response of odd order. An odd impulse response is not suitable to realize a lowpass because its frequency response has a zero at $\omega = 0$. If the filter order is even, a high quality FIR $\frac{\omega_A}{4}$-lowpass filter will have coefficients that alternate between approximately zero and non-zero values except for the middle one. Therefore, the multiplication according to (13) would effectively lead to just a delay in one path and the advantage of the complex filter approach would disappear.

4 Implementation on a TI TMS320C5416

To demonstrate the operability of our feedback reduction system, we implemented the algorithm on a recent low-cost fixed-point digital signal processor. A stereo input signal is sampled at $f_S = 24$ kHz. Each channel stream is quantized with 16 bits and fed into two FIR filters, one for the real and one for the imaginary part. In parallel, the phase modulation factor $\exp(j\frac{\Delta\omega}{\omega_A}n)$ is updated. After the frequency shift according to (13), the 16 most significant bits contribute to the output signal.

Phase modulation factors are computed using the least-squares-approach of TI's DSPLIB sine implementation. The argument is also stored in 16 bits and is increased by the integer value of

$$S = \frac{\Delta\omega}{\omega_A} \cdot 2^{16} \tag{16}$$

in every step. Thus, the granularity of the frequency shift at $f_S = 24$ kHz is about 0.38 Hz. Incrementing the argument by 2^{14} leads to the corresponding cosine value.

FIR filters were also implemented using TI's DSPLIB. In order to exploit the dynamic range and to avoid calculation overflows, the filter coefficients $h_{LP}(n)$ were scaled according to the L_1 norm. The absolute integer value of any signed 16 bit input sample is below 2^{15}. Thus each FIR filter output is at maximum

$$2^{15} \cdot \sum_{n=0}^{N} |h_{LP}(n)| \,. \tag{17}$$

The weighted sum of real and imaginary path contributes to a worst-case scaling of $2\sqrt{2}$. Hence all filter coefficients are scaled such that this final sum is representable with the internal word width of 31 bits plus sign.

Filter coefficients and phase modulation factors are the same for both stereo channels. The required data memory for the FIR implementation is $4N$ words. The core calculation time of the whole frequency shifter is about $4N + 130$ cycles per sample, requiring about 60 MHz CPU frequency for $N = 512$ and $f_S = 24$ kHz.

Multiplying the filter coefficients by $\cos(\frac{\pi}{2}n)$ or $\sin(\frac{\pi}{2}n)$ may be interpreted as sign-alternating masking of every second coefficient. This allows an alternative implementation saving half of the coefficient memory. The two parallel filters write and read alternatively at half of the clock rate, see figure 5. The corresponding filter coefficients are

$$\begin{aligned} \tilde{h}_R(\nu) &= (-1)^\nu \, h_{LP}(2\nu) \\ \tilde{h}_I(\nu) &= (-1)^\nu \, h_{LP}(2\nu + 1) \qquad \text{in each case } \nu = 0 \ldots \frac{N}{2}. \end{aligned} \tag{18}$$

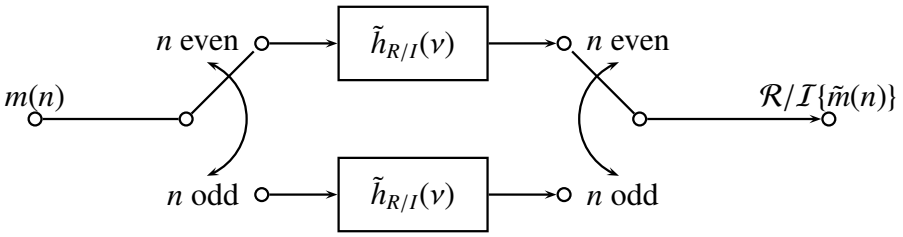

Figure 5: Implementation with reduced memory demand

As practical applications show, frequency shifting reduces the appearance of acoustic feedback. The proposed algorithm yields a well-sounding signal, almost without any distortions. It allows fine adjustable frequency shift and real-time processing. Computational complexity and memory requirements of the described digital fixed-point implementation are quite low.

References

[1] R.W. Guelke and A.D. Broadhurst. Reverberation time control by direct feedback. *Acustica*, 24:33–41, 1971.

[2] C.P. Boner and C.R. Boner. Sound-reinforcing system design. *Applied Acoustics*, 1:115–119, 1968.

[3] Heinrich Kuttruff. *Room Acoustics*. Elsevier Applied Science, 3 edition, 1991.

[4] Johan L. Nielsen and U. Peter Svensson. Performance of some time-varying systems in control of acoustic feedback. *The Journal of the Acoustical Society of America*, 106:240–254, 1999.

[5] Theo A.C.M. Claasen and Wolfgang F.G. Mecklenbräuker. On stationary linear time-varying systems. *IEEE Transactions on Circuits and Systems*, 29:169–184, 1982.

[6] M.R. Schroeder. Improvement of acoustic-feedback stability by frequency shifting. *The Journal of the Acoustical Society of America*, 36(9):1718–1724, 1964.

[7] Andrew Reilly, Gordon Frazer, and Boualem Boashash. Analytic signal generation – tips and traps. *IEEE Transactions on Signal Processing*, 42(11):3241–3245, 1994.